

Modeling protoplanetary disk evolution in young star forming regions

Martijn J. C. Wilhelm¹, Simon Portegies Zwart¹, Claude Cournoyer-Cloutier², Sean Lewis³, Brooke Polak⁴, Aaron Tran⁵, Mordecai-Mark Mac Low^{6,5} and Stephen L. W. McMillan³

¹Leiden Observatory, Leiden University,
P.O. Box 9513, NL-2300 RA, Leiden, the Netherlands
email: wilhelm@strw.leidenuniv.nl

²Department of Physics and Astronomy, McMaster University, Hamilton, Canada

³Department of Physics, Drexel University, Philadelphia, USA

⁴Institut für Theoretische Astrophysik, Zentrum für Astronomie, Universität Heidelberg,
Heidelberg, Germany

⁵Department of Astronomy, Columbia University, New York, USA

⁶Department of Astrophysics, American Museum of Natural History, New York, USA

Abstract. Stars form in clusters, while planets form in gaseous disks around young stars. Cluster dissolution occurs on longer time scales than disk dispersal. Planet formation thus typically takes place while the host star is still inside the cluster. We explore how the presence of other stars affects the evolution of circumstellar disks. Our numerical approach requires multi-scale and multi-physics simulations where the relevant components and their interactions are resolved. The simulations start with the collapse of a turbulent cloud, from which stars with disks form, which are able to influence each other. We focus on the effect of extinction due to residual cloud gas on the early evolution of circumstellar disks. We find that this extinction protects circumstellar disks against external photoevaporation, but these disks then become vulnerable to dynamic truncation by passing stars. We conclude that circumstellar disk evolution is heavily affected by the early evolution of the cluster.

Keywords. methods: numerical, stars: formation, planetary systems: protoplanetary disks, ISM: clouds

1. Introduction

Stars form in clusters through the gravitational collapse of a giant molecular cloud. Gaseous circumstellar disks (often also referred to as protoplanetary disks) are left over from this process, which are dispersed on a time scale of about 10 Myr (Ribas et al. 2014; Michel et al. 2021). Planets form in these disks on a shorter time scale (Tychoniec et al. 2020). The star formation process lasts a few megayears but it takes some 100 Myr for the cluster to dissolve in the Galactic tidal field (Krumholz et al. 2019). The question arises how the dense stellar and gaseous environment affects the evolution of the circumstellar disks, and therewith the planet formation process.

Evidence for a strong interaction between stars and disks is visible in the Orion Nebula Cluster, where several circumstellar disks show comet-like tails directed away from the cluster's most massive star $\theta^1\text{C Ori}$. The material in these tails is being stripped by the radiation of $\theta^1\text{C Ori}$, a process termed external photoevaporation (O'Dell et al. 1993;

Johnstone et al. 1998; Haworth et al. 2018). In a dense stellar environment circumstellar disks can also be stripped during close encounters, a process we'll refer to as dynamic truncation.

Several studies have simulated populations of circumstellar disks in star-forming regions that include the processes of dynamic truncations (Rosotti et al. 2014; Portegies Zwart 2016; Vincke & Pfalzner 2016; Concha-Ramírez et al. 2019a), external photoevaporation (Winter et al. 2019; Nicholson et al. 2019; Parker et al. 2021a,b), or both (Concha-Ramírez et al. 2019b, 2021a,b). In these studies, the initial masses, positions, and velocities of the stars were generally adopted from different observationally motivated parametrizations. The overlap in time scales of the various formation and evolutionary processes, however, requires a more subtle approach in which gas dynamics, star formation, disk evolution, and the various radiative processes are resolved together.

We perform multi-physics simulations based on the Torch model (Wall et al. 2019, 2020), which is assembled using the Astrophysics Multipurpose Software Environment (AMUSE; Portegies Zwart et al. 2009; Pelupessy et al. 2013; Portegies Zwart et al. 2013). Our simulations start with the gravitationally driven hydrodynamical collapse of a giant molecular cloud in which stars form with disks. These disks are subsequently affected by internal and external processes, such as viscous growth, internal and external photoevaporation, and dynamic truncation.

Here we report on a series of ten calculations in which we explore the ecology of circumstellar disks in their star-forming environments. We focus on the effect of extinction by residual gas of the giant molecular cloud (which we'll refer to as the intracluster medium from here on) on the evolution of circumstellar disks. For this reason our runs consist of pairs with identical realizations and star formation procedures, but where we include intracluster extinction in one and neglect it in the other.

2. Method

Our simulations start with the hydrodynamical collapse of a turbulent molecular cloud, in which stars form with disks that are affected by internal and external processes.

2.1. Simulation environment

The collapse of the molecular cloud and star formation are simulated using Torch (Wall et al. 2019, 2020). Torch couples the hydrodynamical adaptive mesh refinement code FLASH ((Fryxell et al. 2000); with additional implementations of radiative transfer (Baczynski et al. 2015), stellar winds, and supernovae) with the stellar dynamics code ph4 (McMillan et al. 2012) and the stellar evolution code SeBa (Portegies Zwart & Verbunt 1996; Toonen et al. 2012), using the AMUSE framework. Gas and stellar dynamics are coupled using the Bridge method (Fujii et al. 2007; Portegies Zwart et al. 2020), adapted to couple between (star) particles and a grid-based distribution of gas.

The circumstellar disk population is simulated using the model of Concha-Ramírez et al. (2021b). Each disk is simulated as a 1D viscous accretion disk using VADER (Krumholz & Forbes 2015), which models accretion onto the host star ($\sim 10^{-8} M_{\odot} \text{ yr}^{-1}$ in our model) and viscous spreading of the disk. The model implements internal and external photoevaporation as extra module. The mass loss through external photoevaporation due to far-UV (FUV) radiation is obtained by interpolation on the FRIED grid (Haworth et al. 2018). In contrast with Concha-Ramírez et al. (2021b) we neglect external photoevaporation due to extreme-UV radiation because their method is difficult to implement when extinction is in play.

Dynamic truncations are implemented with an event-based approach. When two stars pass each other within 0.02 pc, the closest approach between them is estimated as the

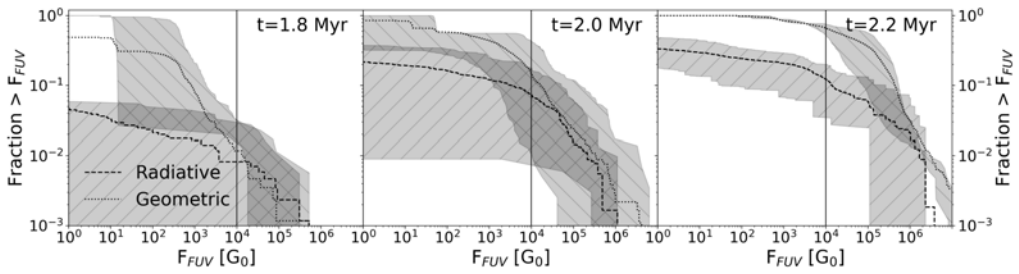


Figure 1. The fraction of circumstellar disks exposed to an FUV radiation field greater than some value, at different moments in time. The dashed curves give runs with the radiative method (including extinction). The dotted curves give runs with the geometric method (without extinction). The vertical lines denote a radiation field of $10^4 G_0$, which is the maximum radiation field on the FRIED grid. The results are aggregated over five simulation runs starting from the same cloud initial conditions, but with different stellar initial mass function realizations. Shaded regions indicate typical run-to-run variation.

periastron of their two-body Keplerian orbit. We subsequently calculate the truncation radius for the disks of both stars following [Portegies Zwart \(2016\)](#). Any disk material beyond the truncation radius is removed.

Each simulation is run twice. In the *radiative* models, in which we account for intracluster extinction, the FUV radiation flux on a specific disk is directly taken from FERVENT, the radiative transfer solver within FLASH. In the *geometric* models, we calculate the local FUV flux by superposing the contribution of each star using the inverse square law. This allows us to study the importance of extinction due to the intracluster medium on the photoevaporation of circumstellar disks.

For efficiency, only $> 7 M_\odot$ stars exert feedback by emitting far (5.6–13.6 eV) and extreme (13.6+ eV) UV radiation, and stellar winds. We refer to these stars as massive stars.

2.2. Initial conditions

The calculations start with a $10^4 M_\odot$ spherical cloud with a Gaussian density profile with a radius of 7 pc. To mediate collapse, the initial cloud is turbulent with a virial ratio (the absolute ratio of kinetic to potential energy) of 0.13. The cloud is embedded in a uniform neutral medium with a number density of hydrogen of 1.25 cm^{-3} . Stars form according to the [Kroupa \(2001\)](#) initial mass function, with masses from $0.08 M_\odot$ to $150 M_\odot$. Each star with mass $M_* < 1.9 M_\odot$ receives a disk upon formation with an initial structure following [Concha-Ramírez et al. \(2021b\)](#), but with a mass $M_d = 0.1 M_\odot (M_*/M_\odot)^{0.73}$, and radius $R_d = 117 \text{ au} (M_*/M_\odot)^{0.45}$ (rescaled from [Wilhelm et al. 2022](#)).

3. Results

Our simulation results are strongly affected by the time of birth, the location, and the velocity of massive stars. Their relative rarity compared to low-mass stars introduces a high degree of stochasticity in our results. To control this, we performed a total of five models (each duplicated) with identical initial hydrodynamical state (i.e., density, temperature, and velocity structure) but with a different random sequence of choices from the stellar initial mass function.

In [Fig. 1](#) we present the fraction of circumstellar disks exposed to an FUV radiation field greater than some value, at 1.8 Myr (just after the massive star has formed in three of five runs), 2.0 Myr (when a massive star has formed in all runs), and 2.2 Myr (which

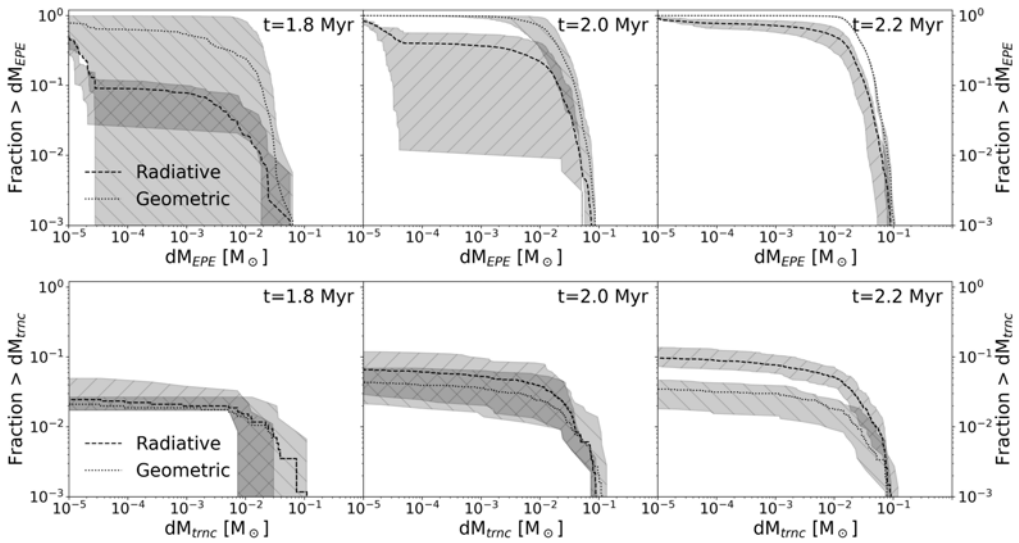


Figure 2. The fraction of circumstellar disks that lost mass through external photoevaporation (top) and dynamic truncation (bottom) greater than some value, for the radiative and geometric method, at different moments in time. The dashed curves give runs with the radiative method (including extinction). The dotted curves give runs with the geometric method (without extinction). The results are aggregated over five simulation runs starting from the same cloud initial conditions, but with different stellar initial mass function realizations. Shaded regions indicate typical run-to-run variation.

four runs have reached). The results are aggregated over all runs where data was present but split by radiation field method. The radiation fields increase with time as the number of massive stars increases. At any time, the radiation field perceived by the stars in the radiative runs is smaller than that in the geometric runs. At 2.2 Myr, on average about 0.4 Myr after the first massive star has formed, only $\sim 30\%$ of disks in the radiative runs are exposed to a FUV radiation field greater than $1 G_0$ ($1.6 \cdot 10^{-3} \text{ erg s}^{-1} \text{ cm}^{-2}$, comparable to the mean interstellar level (Habing 1968)), but $\sim 15\%$ of disks are exposed to a radiation field in excess of $10^4 G_0$. Compare this with the geometric runs, where $\sim 70\%$ of disks are exposed to radiation fields greater than $10^4 G_0$. This implies that the intracluster medium in the parent cloud effectively shields circumstellar disks for at least ~ 0.5 Myr after the formation of the first massive star.

The external radiation field leads to mass loss in the circumstellar disks. The total amount of mass lost in these disks is presented in the top row of panels in Fig. 2. The disks in the geometric runs lose more mass than those in the radiative runs. In the geometric runs at 2.2 Myr, almost every disk has lost $\gtrsim 0.01 M_\odot$ (which is close to all the mass in the disk for the lower-mass stars). At that same time, only half the disks in the radiative runs have lost that amount of material. This demonstrates that the shielding of the intracluster medium effectively protects the circumstellar disks.

The amount of mass lost by dynamic truncation, presented at three moments in time in Fig. 2 (bottom row), shows a reversed trend. More mass is lost by dynamic truncation in the radiative runs than in the geometric runs. At 2.2 Myr, $\sim 10\%$ of disks in the radiative runs have lost $10^{-3} M_\odot$ (or about $1 M_{\text{Jup}}$), against $\sim 3\%$ in the geometric runs. These findings imply that if external photoevaporation is less effective in evaporating disks, the relative importance of dynamic truncation increases.

4. Discussion & conclusion

We have run simulations coupling the formation of stars from a collapsing cloud including massive star feedback, with the evolution of a population of circumstellar disks. We have studied the effect of extinction by residual cloud material on the external photoevaporation of circumstellar disks, and compared the efficiency of this mass loss channel to dynamic truncation due to stellar encounters.

Intracluster extinction effectively shields circumstellar disks from FUV radiation and hence reduces mass loss from external photoevaporation. For example, by ~ 0.5 Myr after the formation of the first massive star, virtually all disks in the geometric runs are exposed to radiation fields in excess of the mean interstellar level, as opposed to $\sim 30\%$ of disks in the radiative runs. Due to disks retaining larger radii, the mass lost through dynamic truncations increases, compared to the case without extinction. However, for the majority of disks the mass loss through external photoevaporation is still greater than through dynamic truncation.

In our simulations, which include feedback by stars more massive than $7 M_{\odot}$, this gas has not been cleared for at least ~ 0.5 Myr after the formation of the first massive star. Our simulation does not include protostellar outflows, which are produced by stars of all masses. While less energetic than feedback from massive stars, this can clear out the neighborhood of stars with disks prior to when massive star feedback becomes effective, decreasing the effectiveness of shielding.

In the radiative runs, $\sim 10\%$ of disks lose $> 1 M_{\text{JUP}}$ through dynamic truncations, compared to $\sim 3\%$ of disks in the geometric runs. However, this depends on the dynamics of newly formed stars, which are spawned from their parent sink particle with a random uniform position offset of up to 0.17 pc and a normally distributed velocity offset proportional to the sink's sound speed ($1.9 \cdot 10^4$ cm s $^{-1}$). Resolving this numerical issue would require the formation of individual stars, which requires increased numerical resolution.

The relative time and distance with respect to massive stars considerably affect circumstellar disk evolution, even on the short time scale of planet formation. It would be interesting to investigate if and how the formation of planets is affected by these environmental variations in disk evolution.

Acknowledgements

The simulations in this work have been carried out on the Cartesius supercomputer, hosted by the Dutch national high performance computing center SURFsara.

This work could not have been done without the help of the AMUSE community and the entire Torch team. We thank Steven Rieder and Inti Pelupessy for their continuing work on AMUSE, and the rest of the Torch team (including Sabrina Appel, William Farner, Joe Glaser, Ralf Klessen, and Alison Sills) for many interesting discussions and a very pleasant collaboration.

References

- Baczynski, C., Glover, S. C. O. & Klessen, R. S. 2015, *MNRAS*, 454, 1
 Concha-Ramírez, F., Vaher, E. & Portegies Zwart 2019a, *MNRAS*, 482, 1
 Concha-Ramírez, F., Wilhelm, M. J. C., Portegies Zwart, S. & Haworth, T. 2019b, *MNRAS*, 490, 4
 Concha-Ramírez, F., Wilhelm, M. J. C., Portegies Zwart, S., van Terwisga, S. E. & Hacar, A. 2021a, *MNRAS*, 501, 2
 Concha-Ramírez, F., Portegies Zwart, S. & Wilhelm, M. J. C. 2021b, *ArXiv* 2101.07826
 Fryxell, B., Olson, K., Ricker, P., Timmes, F. X., Zingale, M., Lamb, D. Q., MacNeice, P., Rosner, R., Truran, J. W. & Tufo, H. 2000, *ApJS* 131, 1
 Fujii, M., Iwasawa, M., Funato, Y. & Makino, J. 2007, *PASJ* 59, 6

- Habing, H.-J. 1968, *Bulletin of the Astronomical Institutes of the Netherlands* 19
- Haworth, T. J., Clarke, C. J., Rahman, W., Winter, A. J. & Facchini, S. 2018, *MNRAS* 481, 1
- Johnstone, D., Hollenbach, D. & Bally, J. 1998, *ApJ* 499, 2
- Kroupa, P. 2001, *MNRAS* 322, 2
- Krumholz, M. R. & Forbes, J. C. 2015, *Astronomy and Computing*, 11
- Krumholz, M. R., McKee, C. F. & Bland-Hawthorn, J. 2019, *ARAA* 57
- McMillan, S., Portegies Zwart, S., van Elteren, A. & Whitehead, A. 2012, *ASP-CS* 453
- Michel, A., van der Marel, N. & Matthews, B. C. 2021, *ApJ* 921, 1
- Nicholson, R. B., Parker, R. J., Church, R. P., Davies, M. B., Fearon, N. M. & Walton, S. R. J. 2019, *MNRAS* 485, 4
- O'Dell, C. R., Wen, Z. & Hu, X. 1993, *ApJ* 410
- Parker, R. J., Nicholson, R. B. & Alcock, H. L. 2021a, *MNRAS* 502, 2
- Parker, R. J., Alcock, H. L., Nicholson, R. B., Panić, O. & Goodwin, S. P. 2021b, *ApJ* 913, 2
- Pelupessy, F. I., van Elteren, A., de Vries, N., McMillan, S. L. W., Drost, N. & Portegies Zwart, S. F. 2013, *A&A* 557
- Portegies Zwart, S. F., Verbunt, F. 1996, *A&A* 309
- Portegies Zwart, S. et al. 2009, *New Astron.* 14, 4
- Portegies Zwart, S., McMillan, S. L. W., van Elteren, A., Pelupessy, I. & de Vries, N. 2013, *Computer Physics Communications*, 184, 3
- Portegies Zwart, S. F. 2016, *MNRAS* 457, 1
- Portegies Zwart, S., Pelupessy, I., Martínez-Barbosa, C., van Elteren, A. & McMillan, S. 2020, *Communications in Nonlinear Science and Numerical Simulations* 85
- Ribas, A., Merin, B., Bouy, H. & Maud, L. T. 2014, *A&A* 561
- Rosotti, G. P., Dale, J. E., de Juan Ovelar, M., Hubber, D. A., Kruijssen, J. M. D., Ercolano, B. & Walch, S. 2014, *MNRAS* 441, 3
- Toonen, S., Nelemans, G., Portegies Zwart, S. 2012, *A&A* 546
- Tychoniec, L., Manara, C. F., Rosotti, G. P., van Dishoeck, E. F., Cridland, A. J., Hsieh, T.-H., Murillo, N. M., Segura-Cox, D., van Terwisga, S. E. & Tobin, J. J. 2020, *A&A* 640
- Vincke, K. & Pfalzner, S. 2016, *ApJ* 828, 1
- Wall, J. E., McMillan, S. L. W., Mac Low, M.-M., Klessen, R. S. & Portegies Zwart, S. 2019, *ApJ* 887, 1
- Wall, J. E., Mac Low, M.-M., McMillan, S. L. W., Klessen, R. S., Portegies Zwart, S., Pellegrino, A. 2020, *ApJ* 904, 2
- Wilhelm, M. J. C. & Portegies Zwart, S. 2022, *MNRAS* 509, 1
- Winter, A. J., Clarke, C. J., Rosotti, G. P., Hacar, A. & Alexander, R. 2019, *MNRAS* 490, 4

Discussion

ORTEGIES ZWART: If you go to [the figure showing the evolution of the radiation field], on the far left you see that the [line indicating no extinction] crosses the [line indicating extinction] near a G_0 of about 10^4 or so. Why do they cross?

WILHELM: That is a result of the resolution. In the case with extinction I get the radiation from different cells in the AMR grid whereas with no extinction I calculate it from the actual distance between the stars. When you get stars that are very close together they might be within the same cell and you get some inaccuracies. It's not going to have an impact on the final results because radiation fields greater than $10^4 [G_0]$ are nearest neighbor extrapolated to the [FRIED] grid which is at $10^4 [G_0]$, so all of these disks actually effectively experience radiation fields of $10^4 [G_0]$.